Electrodeposition Mechanisms and Electrochemical Behavior of Poly(3,4-ethylenedithiathiophene)

H. Randriamahazaka*

Interfaces, Traitements, Organisation et Dynamique des Systèmes (ITODYS), CNRS−UMR 7086, Université Paris 7−Denis Diderot, 1 rue Guy de la Brosse, 75005 Paris, France

G. Sini and F. Tran Van

Laboratoire de Physico-Chimie des Polymères et des Interfaces (LPPI), E.A. 2528, Université de Cergy-Pontoise, 5 mail Gay Lussac, Neuville sur Oise, 95031 Cergy-Pontoise Cedex, France

Received: December 12, 2006; In Final Form: January 25, 2007

The electrodeposition mechanisms of poly(3,4-ethylenedithiathiophene) (PEDTT), which is the sulfur analogue of the well-known poly(3,4-ethylenedioxythiophene) (PEDOT), is investigated in acetonitrile solution by means of potentiostatic methods. By analyzing the current transients within electrocrystallization theory, we observe that the electrodeposition process is a combination of two mechanisms: progressive nucleation, followed by a diffusion-controlled three-dimensional growth (PN3DD); and an instantaneous nucleation, followed by a three-dimensional growth mechanism with charge transfer as the rate-limiting factor (IN3DC). This trend is contrary to PEDOT electrodeposition mechanisms. Cyclic voltametric measurements show important differences between PEDOT and PEDTT. The most unexpected result is that, although 3,4-ethylenedithiathiophene (EDTT) has a lower oxidation potential than 3,4-ethylenedioxythiophene (EDOT), the polymer PEDTT presents a higher oxidation potential and larger band gap than PEDOT. Density functional theory (DFT) calculations reveal important structural and electronic differences between some oligomers of EDTT and EDOT. We analyze these results in terms of the electron-donating effect of the S atom, the difference in the reactivity of the radical-cations of the monomers, and the difference in the geometries of the oligomers.

1. Introduction

Within the field of nanoscience, scientists design new materials to obtain systems that exhibit nonconventional properties.[1] One of the most important features of nanoscience is that the physical and chemical properties of microstructures and nanostructures are often significantly different from those of the same material in the bulk. Thus, the ability to tailor and design microstructures with controlled and confined geometries is essential to meeting technological demands in continuously reduced structural dimensions. One possibility is to design microstructures using conducting polymers. These have attracted great interest recently, because of their potential applications in different technologies (for example, in electrochemical displays, smart windows, sensors, catalysis, redox capacitors, antistatic coatings, electromagnetic shielding, and secondary batteries).[1−4] The possibility of rapidly patterning conducting polymers has been identified as one of the target areas for fabrication of organic electronic and optoelectronic devices.[6−7] Generally, they can be obtained from chemical oxidation or polycondensation via an organometallic route. Another popular method is electrodeposition, mainly from an electrochemical oxidation. Indeed, the electrochemical technique provides a one-step process that does not contain any sophisticated steps of patterning and developing. Accordingly, electrodeposition has attracted considerable interest, because of its technological importance.

Among the organic conducting polymers, poly(3,4-ethylenedioxythiophene) (PEDOT) and its derivatives have attracted great interest, because they seem to be the most chemically stable that are currently available.[8−10] PEDOT can be doped either *n*-type[11−13] or *p*-type.[14−23] Because of the interesting properties of PEDOT, different derivatives have been synthesized to tailor its properties.[9,10,24−26] Our research group is interested in the design of new conducting polymers that display interesting properties (electrochemical stability, high charge storage stability, high electronic conductivity, and low band gap) for several applications, such as in the field of electrochemical devices (sensors, actuators, opto-electronics). Among them, 3,4-ethylenedithiathiophene (EDTT) (see Scheme 1), which is the sulfur analogue of EDOT, is of interest, to investigate the influence of the substituent bridges on the electrochemical behavior of thiophene derivatives. Compared to PEDOT, few papers involve the electrochemical behavior of EDTT and its corresponding polymer, poly(3,4-ethylenedithiathiophene) (PEDTT).[25,27−32] Voltametric measurements show important differences between PEDOT and PEDTT. The most unexpected result is that, although EDTT has a lower oxidation potential than EDOT, the polymer PEDTT presents a higher oxidation potential and larger band gap than PEDOT.

Another intriguing aspect concerns the parameters that control the electrodeposition mechanisms. In the present work, we have investigated the electropolymerization mechanisms of EDTT by means of potentiostatic techniques. Using electrocrystallization theory, we find that the electrodeposition of PEDTT in acetonitrile solution is a combination of two mechanisms: progressive

* Author to whom correspondence should be addressed. Tel: 33 (0)1 44 27 61 07. Fax: 33 (0)1 44 17 68 14. E-mail: randria@itodys.jussieu.fr.

10.1021/jp068525m CCC: $37.00
Published on Web 03/07/2007

SCHEME 1: Synthesis of 3,4-Ethylenedithiathiophene (EDTT)

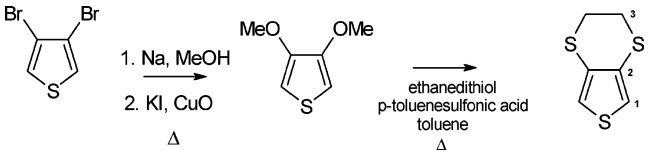

diffusion-controlled three-dimensional nucleation (PN3DD), and an instantaneous charge transfer-limited three-dimensional mechanism (IN3DC). Note that the electrodeposition of PEDOT in acetonitrile follows a combination of instantaneous charge transfer-controlled two-dimensional (IN2DC) and three-dimensional nucleations (IN3DC).[20] To understand these points better, we report, in this paper, the electrochemical behavior of EDTT and PEDTT. Density functional theory (DFT) calculations have also been performed to compare the structural and electronic properties of neutral and cationic EDOT and EDTT monomers and some of their oligomers. Details for the DFT calculations and results are given in the Supporting Information.

2. Experimental Methods

3,4-Ethylenedioxythiophene (EDOT) from Bayer AG was distilled prior to use. Methanol, toluene, cuprous oxide (CuO), potassium iodide (KI), *p*-toluene sulfonic acid, and 3,4-dibromothiophene were obtained from Aldrich. The background electrolyte for the electrodeposition of PEDOT was lithium perchlorate, which was supplied by Fluka. Acetonitrile (high-performance liquid chromatography (HPLC) grade) was obtained from Acros. The synthesis of EDTT is outlined in Scheme 1. 3,4-Dimethoxythiophene was prepared as previously described.[33] 3,4-Dimethoxythiophene was prepared from 3,4-dibromothiophene in 70% yield by exchanging the bromines for methoxy groups in methanol/sodium methoxide, assisted by CuO and a catalytic amount of KI. This compound has previously been trans-etherified with 1,2-dithiol.[34] In our case, it was converted to EDTT with ethenedithiol under standard conditions (catalytic amount of *p*-toluene sulfonic acid in refluxing toluene). The solvent was removed in vacuo, washed with water, dried over $MgSO_4$, and concentrated. The crude product was purified by column chromatography to give EDTT in good yield (40%). ^{13}C NMR analysis confirms its chemical structure: δ (ppm): 118.5 (C1), 125.5 (*C*2), 28.5 (C3).

Electrochemical experiments were performed with a three-compartment three-electrode glass cell. The working electrode was a platinum disk (2.0 mm radius), and platinum wire was used as the counter-electrode. The reference electrode was Ag|AgCl. Electrochemical measurements were performed on an EG&G Princeton Applied Research model 273 Potentiostat/Galvanostat that was controlled by a personal computer (PC), using EG&G Princeton Applied Research model 270 electrochemical software. The working electrode was polished carefully with alumina slurry and cleaned in an ultrasonic bath before each experiment. Prior to all experiments, the solutions were purged with nitrogen, and a nitrogen atmosphere was maintained over the solution during the measurements.

Electropolymerization and deposition were performed at a temperature of 18 ± 1 °C in an acetonitrile solution of 0.01 M monomer and 0.1 M $LiClO_4$ as the supporting electrolyte. The electrode was first stepped from 0.0 to 0.8 V vs Ag|AgCl for a period of ca. 10 s, followed by a second stepping to the polymerization potential. The initial step at 0.8 V vs Ag|AgCl was to allow double-layer charging of the platinum/solution interface; in this way, the effect of double-layer charging was minimized during electropolymerization. Electropolymerization was achieved by a further step to potentials of 1.10−1.20 V vs Ag|AgCl. The thickness of the films can be controlled by varying the duration of the electrodeposition. The nucleation and growth data were fitted using the nonlinear least-squares Marquardt−Levenberg algorithm available in the ORIGIN software (Microcal, Northampton, MA). A minimum of 50 iterations was performed until the fractional change in the χ^2 value was within the tolerance limit, which was set to 0.0005.

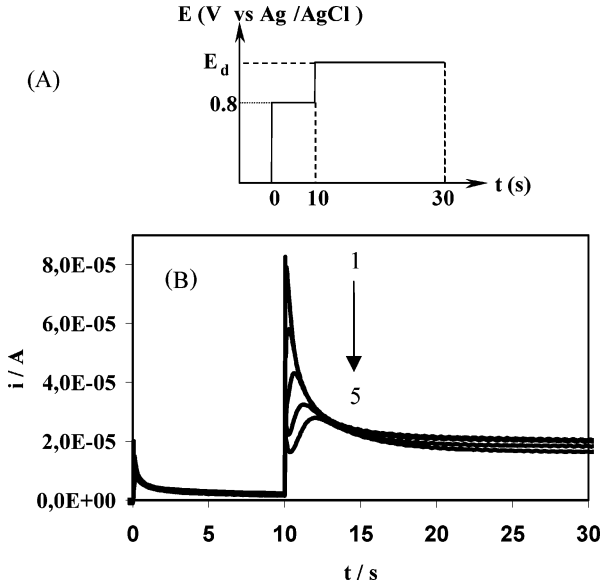

Figure 1. Current−time transients for 0.01 M EDTT during electrooxidation and electropolymerization at different potentials in 0.1 M $LiClO_4$ on a platinum electrode: (A) potential step programs and (B) the variation of the current as a function of time for a deposition potential of 1.18 (curve 1), 1.16 (curve 2), 1.14 (curve 3), 1.12 (curve 4), and 1.11 V (curve 5) vs Ag|AgCl.

3. Results

3.1. Electrodeposition of 3,4-Ethylenedithiathiophene. The cyclic voltammogram (CV) of EDTT in acetonitrile indicates an irreversible behavior. An anodic peak current is observed at 1.25 V vs Ag|AgCl at a scan rate of 0.1 V/s. For the reverse scan, a trace crossing at 1.20 V vs Ag|AgCl is observed. This trace crossing on the reverse sweep in Figure 1 is typical of the first cycle in the voltammograms of compounds that form conducting polymers. Downard and Pletcher[35] called this feature the characteristic nucleation loop and considered it to be proof of the initiation of the nucleation process of the polymer film. However, despite the great facility of electrodeposition of conducting polymers on electrode surfaces, the initial deposition step and the process of propagation of electropolymerization are not clearly understood. Indeed, the electropolymerization mechanisms generally involve many steps. The polymer is generated by a succession of coupling reactions involving radical cations. It has been accepted that electropolymerization proceeds through successive electrochemical and chemical steps, according to a general $E(CE)_n$ scheme.[4,36−40] With EDTT, as in the case of EDOT, the growth of polymer chains occurs exclusively via $\alpha-\alpha$ coupling, because the β or β' positions are blocked by the bridge group. The chemical nature of the bridge group at the β or β' position may influence the electropolymerization and electrodeposition mechanisms. It is well-known that the great stability of oxidized PEDOT is partially due to the presence of the ethylenedioxy bridge that prevents nucleophilic attack at the β or β' positions.

To obtain more information about the electrodeposition mechanisms of EDTT, we performed electropolymerization by a series of potential step experiments in the range of the voltammogram wave where monomer oxidation is observed. Current transient curves during the electrodeposition of EDTT are shown in Figure 1. The general features of these curves are similar to those reported for other conducting polymers.[21,35,40−50] We have analyzed the variation of the current as a function of time for different applied potentials, in terms of nucleation and growth processes, by analogy with the electrodeposition mechanism of the metallic cation.[51−53] The time dependence of the nucleus density, $N(t)$, can be described in terms of the nucleation rate constant k:

$$N(t) = N_0[1 - \exp(-kt)] \tag{1}$$

where both N_0 and k may be dependent on the applied potential. Two limiting cases can be identified. If k is large and $kt \gg 1$ on the time scale of the experiment, then $N(t) \approx N_0$ at all times. This is referred to as instantaneous nucleation (IN), which is equivalent to the site saturation model in solidification. Conversely, if k is small and $kt \ll 1$, then $N(t) = ktN_0$ at sufficiently short times, and the nucleus density increases linearly with time. At longer times, the exponential term in eq 1 dominates, resulting in a saturation of the nucleus density at a value N_0. The growth mechanism may be controlled by the charge transfer or mass transfer. The transients shown in Figure 1 are qualitatively consistent with diffusion-limited growth. However, the nonzero current at long times indicates that other mechanisms may also occur. In other words, the electrodeposition processes involve many mechanisms.

By analogy with nucleation theory for metal deposition, different equations were considered for the fitting of the corresponding currents. In our case, the equation that best fits all the experimental curves is given as follows:

$$i = c[1 - \exp(-dt^2)] + \frac{a}{t^{1/2}}[1 - \exp(-bt^2)] \tag{2}$$

The first term in eq 2 represents an instantaneous nucleation, followed by a three-dimensional growth mechanism with charge transfer as the limiting factor (IN3DC), and the second term corresponds to progressive nucleation, followed by a three-dimensional nucleation under diffusion control (PN3DD). The parameters *a*, *b*, *c*, and *d* are described through the following equations:

$$a = \frac{nFACD^{1/2}}{\pi^{1/2}} \tag{3}$$

$$b = \frac{2}{3}kAN_{\text{diff}}\pi D\left(\frac{8\pi CM}{\rho}\right)^{1/2} \tag{4}$$

$$c = nFAk_3' \tag{5}$$

$$d = \frac{\pi M^2 AN_{3D}k_3^{\,2}}{\rho^2} \tag{6}$$

where n is the number of electrons, F is the Faraday constant, A is the electrode area, D is the diffusion coefficient, C is the bulk concentration of the monomer, k is the rate constant of nucleus formation, N_{diff} is the number of nuclei formed at $t = 0$ with diffusion control, M is the molar mass of the monomer, ρ the density of the monomer, k_3 and k_3' are the rate constants of the three-dimensional nucleus for growth parallel and perpendicular to the surface, and N_{3D} is the number of instantaneous nuclei formed at $t = 0$.

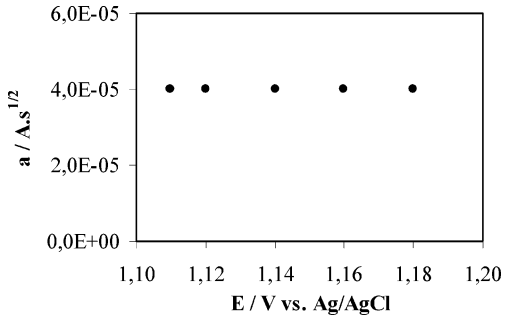

Figure 2. Variation of the parameter *a* for the PN3DD mechanism as a function of potential.

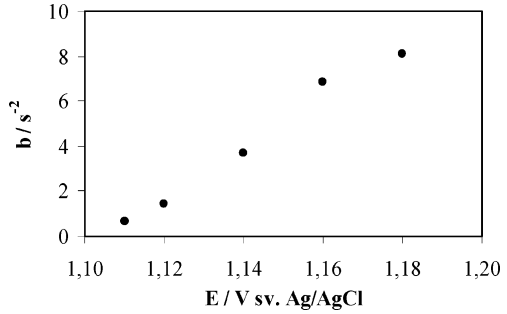

Figure 3. Variation of the parameter *b* for the PN3DD mechanism as a function of potential.

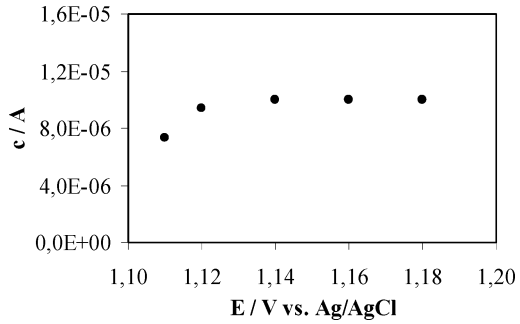

Figure 4. Variation of the parameter *c* for the IN3DC mechanism as a function of potential.

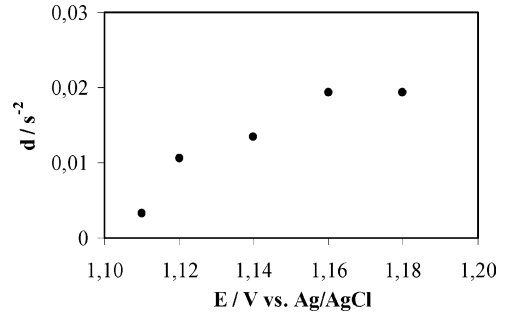

Figure 5. Variation of the parameter *d* for the IN3DC mechanism as a function of potential.

According to the values of the correlation coefficient (>0.99) in each series of experimental data, it can be observed that the model mechanisms involved are the same under our experimental conditions. Therefore, we believe that the chosen models of electrodeposition provide a good basis for the analysis of the electropolymerization of EDTT. Figures 2−5 show the variation of the model parameters as a function of potential.

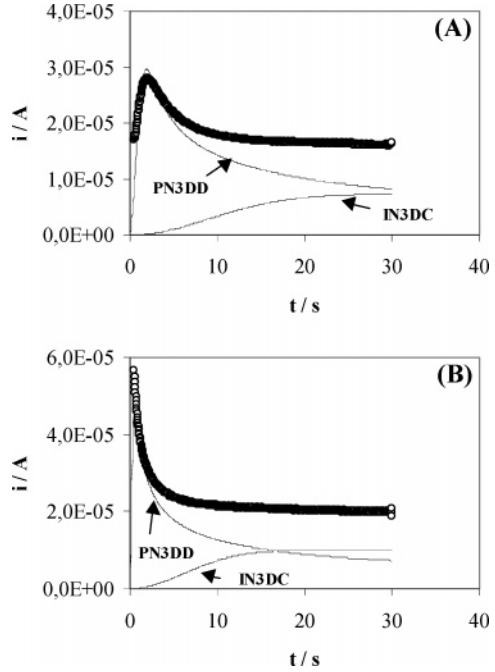

Figure 6. Relative contributions of the PN3DD and the IN3DC mechanisms during the electrodeposition of 0.01 M EDTT in acetonitrile solution containing 0.1 M $LiClO_4$ at (A) 1.11 V and (B) 1.18 V, both vs Ag|AgCl.

We must keep in mind that the parameters *a* and *b* characterize the PN3DD process, and the parameters *c* and *d* describe the IN3DC process. As expected, parameter *a* (eq 3) is not dependent on the applied potential (Figure 2). In Figure 3, we observe an increase in *b*, indicating that the nucleation and growth rates increase with the applied potential. According to eq 4, parameter *b* includes the rate constant of nucleus formation *k* and the number of nuclei N_{diff} formed at $t = 0$ under diffusion control. Indeed, both *k* and N_{diff} may increase with potential; however, at this stage, we are not able to differentiate each evolution. This point will be discussed later. Figure 4 indicates a quasi-constant value of *c*. This behavior indicates that the rate constant k_3' for growth perpendicular to the surface (eq 5) does not vary with the applied potential. Also, we observe a slight increase in parameter *d* (Figure 5). According to eq 6, parameter *d* involves both the rate constant of the three-dimensional nucleus for parallel growth k_3 and the number of instantaneous nuclei N_{3D} formed at $t = 0$. At this stage, we are not able to separate the combined effect of k_3 and N_{3D} on the increase in parameter *d*.

It is well-known that the initial stage of electrodeposition influences the electroactivity of the electrodeposited conducting polymer. With the objective of analyzing this initial stage, we have performed some calculations. Let us examine the relative contribution of each mechanism to the overall processes for different applied potentials. To this end, we calculate the relative contribution of the mechanisms involved with the electrodeposition from eq 2, using the values determined for parameters *a*, *b*, *c*, and *d*. One observes that the PN3DD mechanism is predominant during the initial stage of PEDTT electrodeposition (Figure 6). Figures 7 and 8 show the influence of the applied potential on the individual contributions (for instance, the PN3DD and IN3DC mechanisms). To verify the consistency of these results, we analyze the PN3DD contribution (the first term of eq 2) by determining the maximum current (i_{max}) and

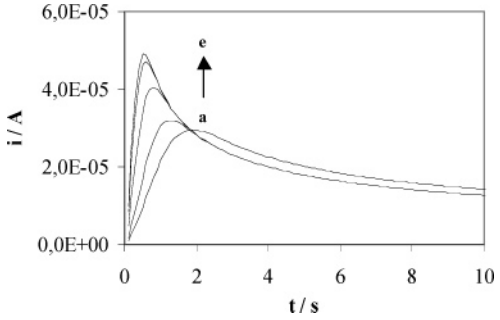

Figure 7. Effect of the applied potential on the PN3DD mechanism during the electrodeposition of 0.01 M EDTT in acetonitrile solution containing 0.1 M $LiClO_4$ for a deposition potential of 1.11 (curve a), 1.12 (curve b), 1.14 (curve c), 1.16 (curve d), and 1.18 V (curve e), all vs Ag|AgCl.

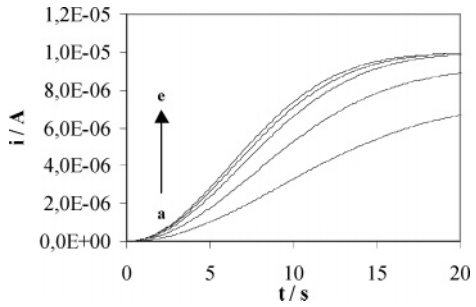

Figure 8. Effect of the applied potential on the IN3DC mechanism during the electrodeposition of 0.01 M EDTT in acetonitrile solution containing 0.1 M $LiClO_4$ for a deposition potential of 1.11 (curve a), 1.12 (curve b), 1.14 (curve c), 1.16 (curve d), and 1.18 V (curve e), all vs Ag|AgCl.

the time at which the this current is obtained (t_{max}). For progressive nucleation and diffusion-limited growth, one has[54]

$$\left(\frac{i}{i_{max}}\right)^2 = 1.2254\left(\frac{t_{max}}{t}\right)\left[1 - \exp\left(-2.3367\frac{t^2}{t_{max}^2}\right)\right] \quad (7)$$

Figure 9 shows reduced parameter plots for PN3DD deposition transients recorded at several potentials. The theoretical curves for progressive nucleation, followed by diffusion-limited growth (solid line), are shown in each graph. In the 1.11−1.18 V potential ranges, the experimental results show good agreement with this model. The PN3DD growth law in the first term of eq 2 assumes that the nucleation rate is constant during deposition. From eq 7, the following relations can be derived for the time and current at the maximum for progressive nucleation and diffusion-limited growth:

$$t_{max} = 3.318D^{-1/2}C^{-1/4}\left(\frac{8\pi M}{\rho}\right)^{-1/4}(kN_{diff})^{-1/2} \quad (8)$$

$$i_{max} = 0.4959nFD^{3/4}C^{9/8}\left(\frac{8\pi M}{\rho}\right)^{1/8}(kN_{diff})^{1/4} \quad (9)$$

If we assume that i_{max} and t_{max} are exponentially dependent, we obtain values of 266 mV/decade and −121 mV/decade for $\{dE/d[\log(i_{max})]\}$ and $\{dE/d[\log(t_{max})]\}$, respectively. From this, a ratio $\{dE/d[\log(i_{max})]\}/\{dE/d[\log(t_{max})]\}$ of −2.2 is obtained. This ratio of −2.2 is similar to the value of −2 obtained from eqs 8 and 9, assuming that kN_{diff} is the only potential-dependent parameter for PN3DD. Based on these data, it can be inferred that, at the initial stage of electrodeposition, the number of oligomers electrodeposited is low and the process is governed by diffusion from the solution. In other words, a high concentra-

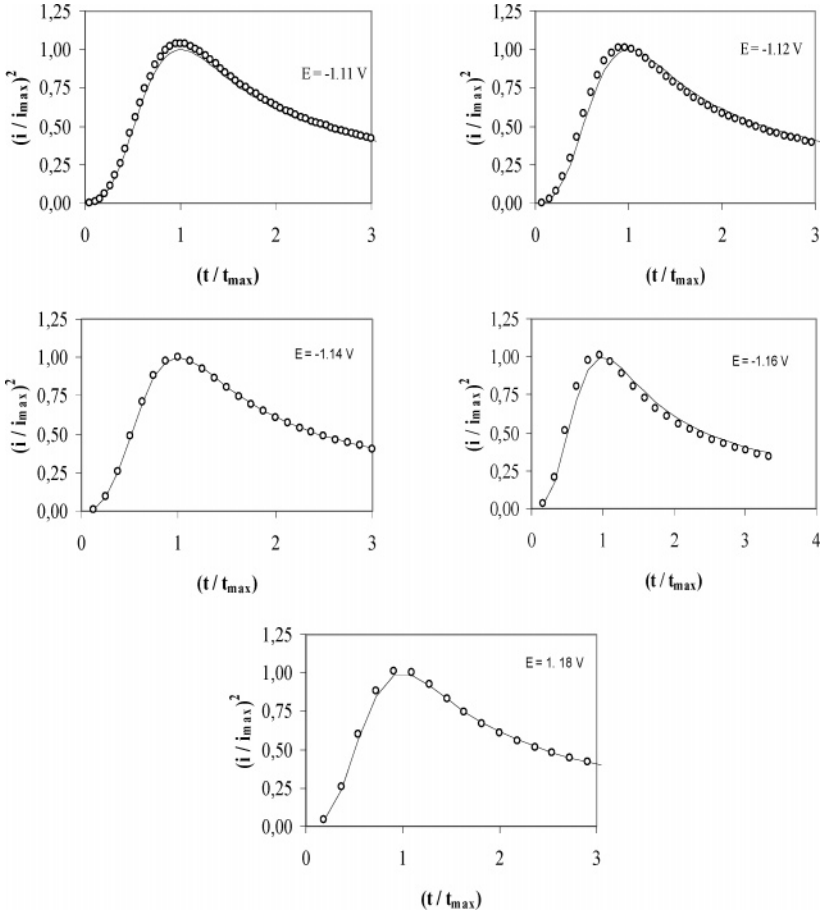

Figure 9. Dimensionless plots of the current transient due to the PN3DD mechanism at different applied potentials during the electrodeposition of 0.01 M EDTT in acetonitrile solution containing 0.1 M $LiClO_4$. In each plot, the solid line corresponds to the calculated curve for progressive nucleation and diffusion-limited growth.

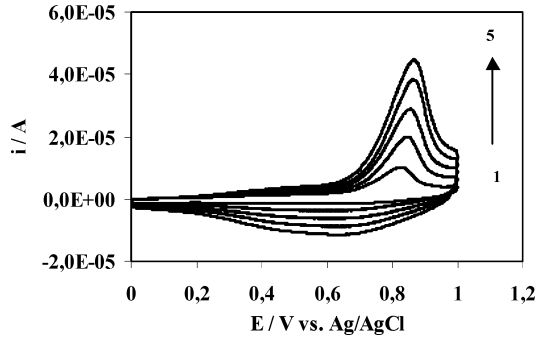

Figure 10. Cyclic voltammograms of PEDTT-modified electrode in 0.1 M $LiClO_4$ acetonitrile solution at different scan rates: 50 (curve 1), 100 (curve 2), 150 (curve 3), 200 (curve 4), and 250 mV/s (curve 5). The charge deposition is 0.53 mC.

tion of soluble oligomers may exist in front of the electrode surface, but the kinetics of the precipitation of the oligomer is initially slow. Progressive nucleation is then observed. As electrodeposition proceeds, the precipitation of the oligomer is no longer the rate-limiting step; the process then becomes rate-controlled by charge-transfer processes. This IN3DC mechanism may involve a coupling reaction between the oligomer radical cation and the monomer radical cation, as reported by Lacroix et al.[40]

3.2. Electrochemical Behavior of a Poly(3,4-ethylenedithiathiophene)-Modified Electrode. Figure 10 shows the cyclic voltammograms of a PEDTT-modified electrode in a monomer-free acetonitrile solution containing 0.1 M $LiClO_4$. One observes a small pre-peak at 0.50 V vs Ag|AgCl, followed by an anodic peak at 0.87 V vs Ag|AgCl. The value of the anodic potential is consistent with the published data.[29] The currents increase with the scan rate υ (data not shown). The scan rate dependence of the currents is linear for scan rates up to ca. 0.25 V/s. This thin-layer behavior indicates a surface-confined electroactive materials and the entire conducting polymer is electroactive on each time scale. To study the influence of the deposition efficiency as a function of time, a series of potentiostatic depositions at 1.20 V vs Ag|AgCl was performed. The maximum capacitance C obtained from the anodic peak current i_p, with $C = i_p/\upsilon$, is dependent on the amount of conducting polymer. We observe a linear variation of C as a function of Q_{dep}. However, a departure from linearity is shown for Q_{dep} up to 1 mC. This behavior seems to indicate that the electrodeposition efficiency decreases. Indeed, we observe a soluble brown compound, probably a soluble oligomer, in front of the electrode surface during the electrodeposition. Also, a change of the electrodeposition mechanisms may occur. These facts can explain the departure from a linear relationship between the maximum capacitance C and Q_{dep}.

Regardless of the exact redox mechanisms, an attempt was made to determine the doping level of PEDTT. The charge density Q_d required for the formation and deposition of the oxidized PEDTT film from monomer can be determined experimentally. If an electrodeposition efficiency of 100% is assumed, this charge density Q_d corresponds to $(2 + \gamma)$ electrons per EDTT unit, where γ is the number of electrons per EDTT required for switching. After electrodeposition, and to obtain the maximum quantity of oxidized polymer, a faradaic charge density Q_{fmax} is needed. The value of Q_{fmax} is determined by

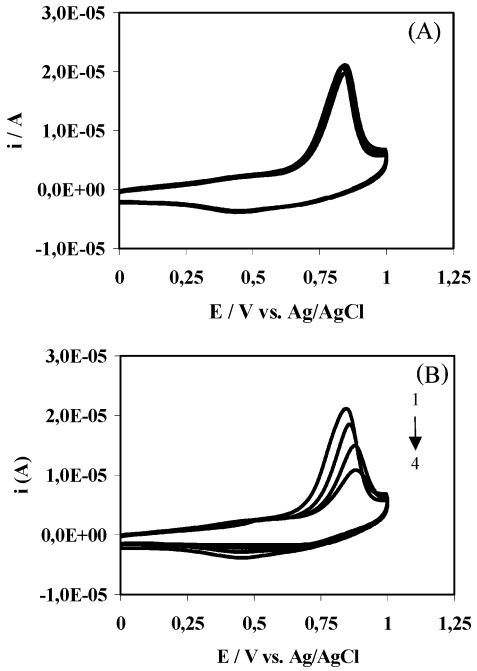

Figure 11. Variation of the cyclic voltammograms of the PEDTT-modified electrode during 150 cycles(A) under nitrogen atmosphere and (B) in the presence of oxygen in 0.1 M $LiClO_4$ acetonitrile solution: the first cycle (curve 1), the 50th cycle (curve 2), the 100th cycle (curve 3), and the 150th cycle (curve 4).

integrating the current during cyclic voltammetric measurement from the initial potential of 0.0 V vs Ag|AgCl to the potential just after the anodic peak at $E_f = 0.95$ V vs Ag|AgCl (see Figure 10). In this potential range, the capacitive charge is assumed to be negligible, compared to the faradaic charge. Thus, γ can be calculated by

$$\gamma = \frac{2}{\left[\frac{Q_d}{Q_{f,max}}\right] - 1} \tag{10}$$

Equation 10 can be rewritten as

$$Q_{f,max} = \left(\frac{\gamma}{2+\gamma}\right) Q_d \tag{11}$$

From eq 11, the variation of $Q_{f,max}$, as a function of Q_d, gives a linear curve with a slope of $\gamma/(2+\gamma)$ (data not shown). By graphical determination, a γ value of 0.1 is obtained. The value of γ is low, compared to that generally observed for thiophene derivatives ($\sim$0.3).[20] Note that this value of γ for PEDTT is probably underestimated, because we assume an electrodeposition efficiency of 100%. Indeed, a soluble oligomer of EDTT is observed during electrodeposition.

We have also studied the electrochemical stability of PEDTT in the presence and absence of oxygen. To this end, successive cycles are performed in a monomer-free solution. In a deoxygenated solution, a decrease in electroactivity of only 15% is observed after 150 cycles at a scan rate of 0.2 V/s (Figure 11A). However, a gradual decrease in the electroactivity is obsevred when oxygen is present in the solution (Figure 11B). This decrease may be due to a nucleophilic reaction between the radical cation in the oxidized polymer and oxygen, as observed for polythiophene.

4. Discussion

It is interesting to compare the present results with our previous work, with regard to the redox properties and the electrodeposition of EDOT.[21] In acetonitrile solution, EDOT displays an anodic peak potential at 1.44 V vs Ag|AgCl at a scan rate of 100 mV/s. The anodic peak of EDTT at 1.25 V vs Ag|AgCl is lower than that of EDOT. This behavior is due to the higher electron-donating effect of S atoms, compared to O atoms in the bridge substituent of the monomer. Using density functional theory (DFT) calculations, we observe that the highest occupied molecular orbital (HOMO) of EDTT is higher (on the absolute energy scale) than that of EDOT (see Table 1 in the Supporting Information). Thus, the ionization potential of EDTT is lower than that of EDOT. However, the oxidation peak potential of PEDTT is lower than that observed in the case of PEDOT. This behavior may be due to the difference in the kinetics of polymer formation, the polymer length, the geometry of the polymers, and the morphology of the deposited materials.

It has been reported that the formation of the oligomer follows radical cation−radical cation coupling (CR−CR).[36,37] The rate of CR−CR coupling increases as the spin density of the carbon in the α-position of the radical cation of the monomer increases. DFT calculations on the radical cations of EDTT and EDOT show a lower α-C spin density for EDTT (see Table 1 in the Supporting Information). Consequently, the rate of oligomer formation from EDTT may be less than that from EDOT. The smaller spin densities at the α-C positions of EDTT oligomers correspond to lower reactivity during the polymerization process, indicating the formation of shorter PEDTT chains than in the case of PEDOT.

It is interesting to focus on the important geometrical difference between these species, ca. oligomers. $(EDOT)_n$ oligomers display a planar geometry, whereas a large twist angle between monomers is observed for $(EDTT)_n$ oligomers (see Figure S2 in the Supporting Information). This behavior, which is due to steric repulsion of the S atoms on the two neighboring ethylenedithia bridges, is in agreement with the inversion of the oxidation peak potential after electropolymerization. In fact, the twisted structure for PEDTT is not appropriate for π-conjugation between oligomer rings, which, in turn, will leave the HOMO energy level almost unchanged during polymerization. On the other hand, the planar structure of PEDOT allows a large mean effective conjugation length, which makes its HOMO energy level increase. It is then easy to understand that, after polymerization, the order of HOMO energy levels is inverted. Thus, despite the lower value of the oxidation potential of EDTT, the peak potential of PEDTT becomes higher than that of PEDOT. As shown in Figure 10, the peak potential of PEDTT is $\sim$0.87 V vs Ag|AgCl, whereas a value of 0.25 V vs Ag|AgCl was observed for PEDOT.[20] These results are also in agreement with the band gaps determined from UV−vis spectroscopy. The onset value of the $\pi-\pi^*$ transition is 2.12 eV for PEDTT and 1.6 eV for PEDOT, which are in good agreement with the published values.[25] The difference of $\sim$0.5 eV in the band gaps of PEDTT and PEDOT may be due to the difference in the morphology of these polymers: the effective π-conjugation in the case of PEDOT makes the highest occupied molecular orbital−lowest unoccupied molecular orbital (HOMO−LUMO) gap decrease during polymerization much greater than that in the case of PEDTT. Calculations show that this gap is greater for EDOT than for EDTT, but smaller for PEDOT than for PEDTT (see Table 2 in the Supporting Information). The variation of the ZINDO/CIS-calculated first excitation energies follows the same trend.

Now we focus on the difference in the electrodeposition mechanisms. As shown previously, the electrodeposition of EDTT follows a combination of two mechanisms: progressive

diffusion-controlled three-dimensional nucleation (PN3DD), and an instantaneous three-dimensional mechanism with charge transfer as the rate-limiting factor (IN3DC). For PEDOT, electrodeposition occurs by instantaneous nucleation and two-dimensional growth (IN2DC), in combination with instantaneous nucleation and three-dimensional growth (IN3DC); both are charge-controlled. This change in the growth mechanisms may reflect the difference in the reactivity of the radical cation, the solubility of the oligomer, and the shape of the nuclei at the beginning of the electrodeposition process. Furthermore, nucleus formation is related to the solubility of the oligomer. The twisted structure of the $(EDTT)_n$ oligomers should favor solubility, and they can inhibit the deposition processes. Indeed, the insolubility of conducting polymers is due to the great van der Waals interactions and the π-stacking between the polymer chains, which are more favorable for planar polymer chains. Because $(EDTT)_n$ oligomers are not planar, their solubility may be expected to be higher than that of the $(EDOT)_n$ oligomer. These behaviors may explain why progressive nucleation occurs during the electrodeposition of EDTT.

It is also important to note that the two-dimensional mechanism is absent from the electrodeposition of EDTT. Indeed, film growth can occur in different ways.[53] If the interactions between the electrode surface and the deposited material are weak, in comparison to those within the deposited material itself, deposition occurs in the form of three-dimensional nuclei (3D island or Volmer−Weber model), which grow and finally coalesce. On the other hand, if there is a strong surface-deposit interaction, the deposits have a tendency to form a two-dimensional adlayer. In this case, if the formation of the adlayer results in a deformation of the deposit structure, three-dimensional growth centers nucleate on the adlayer and, subsequently, growth occurs on these nuclei (a three-dimensional island on a two-dimensional layer or the Stranski−Krastanov model). However, if the deformation is insignificant, the deposit may continue to grow via the addition of successive layers upon each other (layer by layer, or the Frank van der Merwe model). The absence of a two-dimensional mechanism during the electrodeposition of PEDTT is consistent with the geometry of the EDTT oligomer. Indeed, the twisted geometry of the EDTT oligomer should decrease the interactions between the electrode surface and the EDTT oligomer. In the last stage of electrodeposition, the predominant mechanism for both EDTT and EDOT is charge-controlled three-dimensional instantaneous nucleation and growth (IN3DC). These results indicate clearly a modification of the predominant mechanism during the growth process. Also, it has been reported by Lacroix and co-workers[39,40] that, as the oligomer length increases, oligomer−monomer coupling reactions are more favorable than oligomer−oligomer reactions. Moreover, the difference in packing ability may modify the initial stage of the nucleation and growth mechanisms.

Now, if we consider the electrochemical stability, we find that PEDTT is less stable than PEDOT under the same successive cyclic voltammetry (Figure 11B). In the presence of oxygen, this difference is probably due to the difference in the reactivity of the oxidized polymer toward nucleophilic attack. It has been reported that the stability of PEDOT is strongly related to its perfect inter-ring conjugation.[9,11] In view of this factor, one can correlate the lower electrochemical stability of PEDTT with its nonplanarity. Because of its twisted structure, PEDTT should present a much more porous structure than PEDOT and a greater specific surface area, consequently increasing its chemical reactivity. As has been reported previously, oxidation of the sulfur group may occur during the over-oxidation of polythiophene.[54] Accordingly, a sulfone or sulfoxide may be generated in the thiophene ring of PEDTT during its oxidation in the presence of oxygen.

5. Conclusion

We have shown that the chemical nature of the bridge group at the β or β' positions of the thiophene ring has an important role in the polymerization and electrodeposition of thiophene derivatives. The spin density on the α-carbons of the radical cation of 3,4-ethylenedithiathiophene (EDTT) and its oligomer is lower than that for 3,4-ethylenedioxythiophene (EDOT). This fact decreases the reactivity of EDTT (and its oligomer) radical cation and induces a lower degree of polymerization for poly(3,4-ethylenedithiathiophene) (PEDTT). Density functional theory (DFT) calculations clearly show that the twisted geometry of the PEDTT oligomers profoundly affects the inter-ring conjugation properties, which, in turn, should affect the chemical stability. On the other hand, the twisted structure of PEDTT modifies the electrodeposition mechanisms. Using electrocrystallization theory, we can interpret the electrodeposition of PEDTT using a combination of two mechanisms: progressive diffusion-controlled three-dimensional nucleation (PN3DD), and an instantaneous three-dimensional mechanism with charge transfer as the limiting factor (IN3DC).

Recently, much research has been concerned with the patterning of conductive polymer films. The results presented in this work indicate that analysis of the electronic properties of the monomer and the corresponding oligomer is of interest for a better understanding of the electrochemical properties of electrodeposited conducting polymers. Indeed, polymeric integrated circuits are rapidly growing in importance for building thin, flexible, and inexpensive electronic circuits. Also, potential applications of polymeric integrated circuits range from low-end to high-volume microelectronics.

Acknowledgment. This work was supported by the French Ministry of Research. The authors are particularly grateful to Dr. J. S. Lomas (ITODYS, University Paris 7), who kindly revised our text and helped us to put it into correct English.

Supporting Information Available: Cyclic voltammograms of 0.01 M EDTT in acetonitrile solution with 0.1 M $LiClO_4$ on a platinum electrode, graphic depictions of the ring structure, details regarding DFT calculations and results, and associated references. (PDF) This material is available free of charge via the Internet at http://pubs.acs.org.

References and Notes

(1) Roncali, J. *Chem. Rev.* **1992**, *92*, 711.
(2) Nalwa, H. S., Ed. *Handbook of Conductive Molecules and Polymers*, Vols. 1−4; Wiley, New York, 1997.
(3) Heeger, A. J. *J. Phys. Chem. B* **2001**, *105*, 8475.
(4) MacDiarmid, A. G. *Angew. Chem., Int. Ed.* **2001**, *40*, 2581.
(5) Gates, B. D.; Xu, Q.; Stewart, M.; Ryan, D.; Willson, C. G.; Whitesides, G. M. *Chem. Rev.* **2005**, *105*, 1171.
(6) Sirringhaus, H.; Tessler, N.; Friend, R. H. *Science* **1998**, *280*, 1741.
(7) Holdcroft, S. *Adv. Mater.* **2001**, *13*, 1753.
(8) Heywang, G.; Jonas, F. *Adv. Mater.* **1992**, *4*, 116.
(9) Groenendaal, B. L.; Jonas, F.; Freitag, D.; Pielartzik, H.; Reynolds, J. R. *Adv. Mater.* **2000**, *12*, 481.
(10) Kvarnström, C.; Neugebauer, H.; Ivaska, A.; Sariciftci, N. S. *J. Mol. Struct.* **2000**, *521*, 271.
(11) Ahonen, H. J.; Lukkari, J.; Kankare, J. *Macromolecules* **2000**, *33*, 6787.
(12) Skompska, M.; Mieczkowski, J.; Holze, R.; Heinze, J. *J. Electroanal. Chem.* **2005**, *577*, 9.
(13) Dietrich, M.; Heinze, J.; Heywang, G.; Jonas, F. *J. Electroanal. Chem.* **1994**, *369*, 87.

(14) Yamato, H.; Ohwa, M.; Wernet, W. *J. Electroanal. Chem.* **1995**, *397*, 163.
(15) Sotzing, G. A.; Reynolds, J. R. *Chem. Mater.* **1996**, *8*, 882.
(16) Fu, Y.; Cheng, H.; Elsenbaumer, R. L. *Chem. Mater.* **1997**, *9*, 1720.
(17) Carlberg, J. C.; Inganäs, O. *J. Electrochem. Soc.* **1997**, *144*, L61.
(18) Huchet, L.; Akoudad, S.; Roncali, J. *Adv. Mater.* **1998**, *10*, 541.
(19) Sakmeche, N.; Aeiyach, S.; Aaron, J. J.; Jouini, M.; Lacroix, J. C.; Lacaze, P. C. *Langmuir* **1999**, *15*, 2566.
(20) Randriamahazaka, H.; Noël, V.; Chevrot, C. *J. Electroanal. Chem.* **1999**, *472*, 103; *J. Electroanal. Chem.* **1999**, *476*, 183 (erratum).
(21) Xia, C.; Advincula, R. C.; Baba, A.; Knoll, W. *Langmuir* **2002**, *18*, 3555.
(22) Li, C.; Imae, T. *Macromolecules* **2004**, *37*, 2411.
(23) Seshadri, V.; Wu, L.; Sotzing, G. A. *Langmuir* **2003**, *19*, 9479.
(24) Groenendaal, L. B.; Zotti, G.; Aubert, P. H.; Waybright, S. M.; Reynolds, J. R. *Adv. Mater.* **2003**, *15*, 855.
(25) Turbiez, M.; Frère, P.; Allain, M.; Gallego-Planas, N.; Roncali, J. *Macromolecules* **2005**, *38*, 6806.
(26) Segura, J. L.; Gomez, R.; Reinold, E.; Bauerle, P. *Org. Lett.* **2005**, *7*, 2345.
(27) Wang, C.; Schindler, J. L.; Kannewurf, C. R.; Kanatzidis, M. G. *Chem. Mater.* **1995**, *7*, 58.
(28) Pozo-Gonzalo, C.; Khan, T.; McDouall, J. J. W.; Skabara, P. J.; Roberts, D. M.; Light, M. E.; Coles, S. J.; Hursthouse, M. B.; Neugebauer, H.; Cravino, A.; Sariciftci, N. S. *J. Mater. Chem.* **2002**, *12*, 500.
(29) Blanchard, P.; Cappon, A.; Levillain, E.; Nicolas, Y.; Frere, P.; Roncali, J. *Org. Lett.* **2002**, *4*, 607.
(30) Spencer, H. J.; Berridge, R.; Crouch, D. J.; Wright, S. P.; Giles, M.; McCulloch, I.; Coles, S. J.; Hursthouse, M. B.; Skabara, P. J. *J. Mater. Chem.* **2003**, *13*, 2075.
(31) Spencer, H. J.; Skabara, P. J.; Giles, M.; McCulloch, I.; Coles, S. J.; Hursthouse, M. B. *J. Mater. Chem.* **2005**, *15*, 4783.
(32) Cravino, A.; Neugebauer, H.; Petr, A.; Skabara, P. J.; Spencer, H. J.; McDouall, J. J.W.; Dunsch, L.; Sariciftci, N. S. *J. Phys. Chem. B* **2006**, *110*, 2662.
(33) Langeveld-Voss, B. M. W.; Janssen, R. A. J.; Meijer, E. W. *J. Mol. Struct.* **2000**, *521*, 285.
(34) Goldoni, F., Langeveld-Voss, B. M., Meijer, E. W. *Synth. Commun.* **1998**, *28*, 2237.
(35) Downard, A. T.; Pletcher, D. *J. Electroanal. Chem.* **1986**, *206*, 147.
(36) Audebert, P.; Hapiot, P. *Synth. Met.* **1995**, *75*, 95.
(37) Andrieux, C. P.; Audebert, P.; Hapiot, P.; Saveant, J. M. *J. Phys. Chem.* **1991**, *95*, 10158.
(38) Smith, J. R.; Ratcliffe, N. M.; Cox, P. A.; Campbell, S. A. *J. Chem. Soc., Faraday Trans.* **1995**, *91*, 2331.
(39) Lacroix, J. C.; Valente, R. J.; Maurel, F.; Lacaze, P. C. *Chem.—Eur. J.* **1998**, *4*, 1667.
(40) Lacroix, J. C.; Maurel, F.; Lacaze, P. C. *J. Am. Chem. Soc.* **2001**, *123*, 1989.
(41) Asavapiriyanont, S.; Chandler, G. K.; Gunawardena, G. A.; Pletcher, D. *J. Electroanal. Chem.* **1984**, *177*, 229 and 245.
(42) Hillman, A. R.; Mallen, E. F. *J. Electroanal. Chem.* **1987**, *220*, 351.
(43) Hillman, A. R.; Swann, M. J. *Electrochim. Acta* **1988**, *33*, 1303.
(44) Li, F.; Albery, W. J. *Electrochim. Acta* **1992**, *37*, 393.
(45) Bade, K.; Tsakova, V.; Schultze, J. W. *Electrochim. Acta* **1992**, *37*, 2255.
(46) Chao, F.; Costa, M.; Tian, C. *Synth. Met.* **1993**, *53*, 127.
(47) Cordova, R.; del Valle, M. A.; Arratia, A.; Gomez, H.; Schrebler, R. *J. Electroanal. Chem.* **1994**, *377*, 75.
(48) Lukkari, J.; Alanko, M.; Pitkänen, V.; Kleemola, K.; Kankare, J. *J. Phys. Chem.* **1994**, *98*, 8525.
(49)) Kontturi, K.; Pohjakallio M.; Sundholm G.; Vieil, E. *J. Electroanal. Chem.* **1995**, *384*, 67.
(50) Schrebler, R.; Grez, P.; Cury, P.; Veas, C.; Merino, M.; Gomez, H.; Cordova, R.; del Valle, M. A. *J. Electroanal. Chem.* **1997**, *430*, 77.
(51) Fleischmann, M.; Thirsk, H. R. *Trans. Faraday Soc.* **1955**, *51*, 71.
(52) Southampton Electrochemistry Group. *Instrumental Methods in Electrochemistry*, Ellis Horwood: Chichester, U.K., 1985.
(53) Budevski, E.; Staikov, G.; Lorenz, W. J. *Electrochemical Phase Formation and Growth*; VCH: Weinheim, Germany, 1996.
(54) Barsch, U.; Beck, F. *Electrochim. Acta* **1996**, *41*, 1761.